High Sensitivity of Stark-Shift Voltage-Sensing Dyes by One- or Two-Photon Excitation Near the Red Spectral Edge

Bernd Kuhn,* Peter Fromherz,[†] and Winfried Denk*

*Department for Biomedical Optics, Max Planck Institute for Medical Research, Heidelberg, Germany; and
[†]Department of Membrane and Neurophysics, Max Planck Institute of Biochemistry, Martinsried/Munich, Germany

ABSTRACT   Sensitivity spectra of Stark-shift voltage sensitive dyes, such as ANNINE-6, suggest the use of the extreme red edges of the excitation spectrum to achieve large fractional fluorescence changes with membrane voltage. This was tested in cultured HEK293 cells. Cells were illuminated with light at the very red edge of the dye's excitation spectrum, where the absorption cross section is as much as 100 times smaller than at its peak. The small-signal fractional fluorescence changes were $-0.17\%/mV$, $-0.28\%/mV$, and $-0.35\%/mV$ for one-photon excitation at 458 nm, 488 nm, and 514 nm, respectively, and $-0.29\%/mV$, $-0.43\%/mV$, and $-0.52\%/mV$ for two-photon excitation at 960 nm, 1000 nm, and 1040 nm, respectively. For large voltage swings the fluorescence changes became nonlinear, reaching 50% and -28% for 100 mV hyper- and depolarization, respectively, at 514 nm and 70% and -40% at 1040 nm. Such fractional sensitivities are ~5 times larger than what is commonly found with other voltage-sensing dyes and approach the theoretical limit given by the spectral Boltzmann tail.

INTRODUCTION

Voltage-sensitive dyes (VSDs) are widely used for probing cellular membrane potentials (London et al., 1987; Grinvald et al., 1988; Meyer et al., 1997; Spors and Grinvald, 2002), but for dyes fast enough to measure neural signals the fractional fluorescence changes are rather small, compared to, for example, Ca^{2+} indicators. To overcome shot noise and achieve a sufficient signal-to-noise ratio (SNR) high fluorescence intensities are, therefore, needed. This, in turn, leads to photodynamic damage and quick photobleaching. This problem becomes increasingly more serious as spatial and temporal resolutions need to be increased and has prevented the application of VSD recordings to problems such as spike time synchronization (Singer, 1999; Salinas and Sejnowski, 2001), where VSDs would otherwise be the preferred tool. The amount of fluorescence light that is necessary to achieve a particular SNR for a given membrane voltage decreases strongly as the relative fluorescence change per unit of voltage change increases. An increase in that sensitivity will, therefore, reduce photodamage substantially. The voltage sensitivity is a function of the intrinsic properties of the dye, such as the size of the spectral shift, and can be particularly sensitive to the choice of excitation wavelength with the maximal sensitivity at the spectral edge as has been realized early on and demonstrated for a limited wavelength range (Loew, 1982). In this article we demonstrate that the sensitivity becomes even larger at extreme wavelengths and approaches the thermodynamic voltage-sensitivity limit. There we took advantage of the recent synthesis of a new class of VSDs (Hübener et al., 2003), which shows a spectral change that is entirely due to the molecular Stark effect (Kuhn and Fromherz, 2003). In addition, the charge shift between ground and excited state, on which the spectral shift directly depends, is nearly twice as large for ANNINE-6 compared to the classical styryl dye di-4-ANEPBS (Fluhler et al., 1985; Kuhn and Fromherz, 2003). In this article we show that the dye's sensitivity can be increased beyond the already high values shown in the initial characterization (Kuhn and Fromherz, 2003) by using excitation wavelengths at the extreme long-wavelength edge of the absorption spectrum by both one- and two-photon excitation (Denk et al., 1990).

EXPERIMENTAL METHODS

Cell culture

HEK293 cells (DSMZ GmbH, Braunschweig, Germany) were cultured using standard methods on glass coverslips (diameter 24 mm, Assistent, Glaswarenfabrik Karl Hecht KG, Sondheim, Germany). The coverslips were coated with fibronectin (No. 68885, Boehringer-Mannheim, Germany) in PBS (140 mM NaCl, 2.7 mM KCl, 1.5 mM KH_2PO_4, 6.5 mM $Na_2HPO_4 \times 2H_2O$) by incubation for 45 min in a 10 μg/ml fibronectin solution and a single subsequent wash with PBS. The cells were plated at densities of 15,000 cells per coverslip and were used for up to 3 days after plating while the cell density was still low. All measurements were done in a Ringer solution containing (in mM) 135 NaCl, 5.4 KCl, 1.0 $MgCl_2$, 1.8 $CaCl_2$ and 5.0 Hepes, adjusted to pH 7.2 with NaOH.

Staining

ANNINE-6 (Fig. 1 *a*) was dissolved in a solution of 20% Pluronic F-127 DMSO (P-3000, Molecular Probes, Eugene, Oregon) at a concentration of 0.5 mg/ml and sonicated for 15 min. The glass coverslip with the HEK293 cells was taken out of the culture well, exposed to the staining solution (dye stock solution diluted 1:100 into Ringer) for 5 min and finally washed with pure Ringer solution.
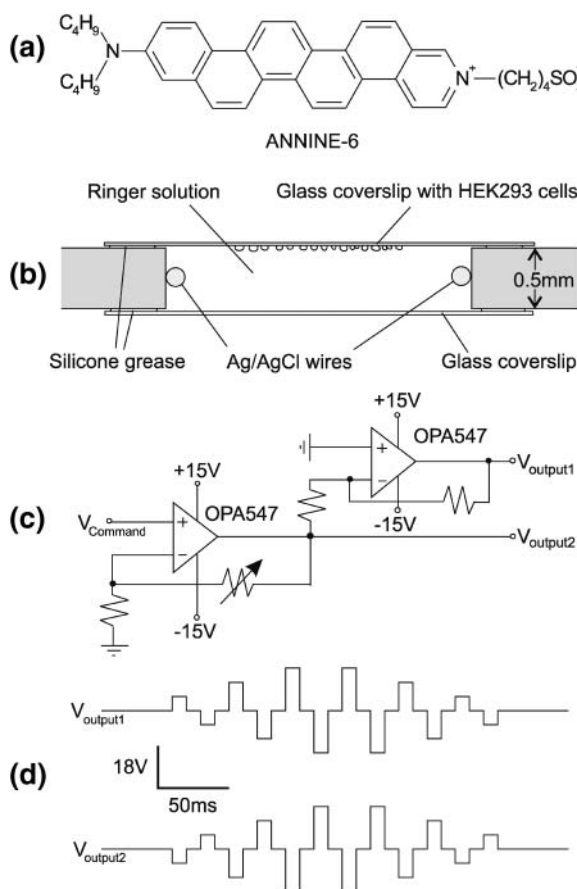
FIGURE 1 (*a*) Structure of ANNINE-6, a completely anellated hemi-cyanine dye. (*b*) Cross-sectional view of the electric-field application chamber. Ringer solution flows perpendicular to the paper plane. (*c*) Amplification circuit used to apply the electric fields. (*d*) Voltage pulse protocol.

Electric-field application

To change the voltage across the cell membrane we applied an extracellular electric field. This method (Gross et al., 1986) has a somewhat reduced voltage calibration accuracy but is much simpler than whole-cell recordings, for example, permitting the transfer of the recording chamber between microscope setups thereby allowing the exploration of a wider parameter range. Our custom-made chamber (Fig. 1 *b*) consists of a 2.6 mm wide, and 30 mm long slit in a 0.5 mm thick PMMA (Plexiglas) plate. Two chlorided silver wires (diameter 0.127 mm, Cat. No. 7860, A-M Systems, INC., Everett, WA) for the application of the electrical field were fixed to the long edges of the channel with two-component epoxy resin glue (plus sofortfest, UHU, Bühl, Germany). This chamber was sealed on the bottom with a clean coverslip (24 mm × 50 mm) attached with silicone grease (Bayer-silicone, Bayer AG, Leverkusen, Germany). The coverslip with the stained HEK293 cells was dried around the edges to get a watertight seal with silicone grease and then mounted cells down on the top side of the chamber. Two openings allowed the continuous perfusion (~2 ml/min) with physiological saline using a gravity-fed perfusion system.

The voltage stimuli were generated by an arbitrary waveform generator (model 395, wavetek, Ismaning, Germany) and amplified by a custom-built push-pull circuit (using two operational amplifiers, OPA547, Texas Instruments Inc., Texas, USA, Fig. 1 *c*). To avoid electrolysis at the electrodes and ionophoresis of cell-surface components all applied voltage waveforms were purely AC. Short pulses were used to minimize heating

(Fig. 1 *d*). The application of the pulse protocol was synchronized to the start of line scan acquisition.

Whole-cell tight-seal voltage-clamp recordings on HEK293 cells were performed using pipettes with a resistance of ~6 MOhm and an epc9 amplifier (HEKA, Göttingen, Germany).

Imaging

For one-photon excitation we used laser scanning microscopes (Zeiss LSM 510 NLO and Leica TCS SP2) with Ar-ion laser excitation (458 nm, 488 nm, or 514 nm). We used laser illumination instead of, for example, Xe arc-lamps because narrow spectral width and high intensities are needed to obtain sufficient excitation of the dye at the spectral edge. The excitation light at the Zeiss microscope was coupled in via the main dichroic beam splitters (HFT 458/514, reflecting the 458 nm and 514 nm laser lines or HFT KP 700/488, a combined 700 nm short pass and 488 nm reflector). The emitted light was filtered by a long-pass filter (LP560). The Leica microscope uses an acousto-optical main beam splitter and fluorescence was collected in the range of 520 nm to 800 nm. The maximal excitation intensities at the sample were for the Zeiss (Leica) microscope: 1.3 mW (1.5 mW) at 514 nm, 200 μW (250 μW) at 488 nm and 28 μW (35 μW) at 458 nm. The pinhole was completely opened up (8.5 airy units) to collect as much light as possible. A Zeiss IR 40x /0.8 water immersion objective was used at the Zeiss microscope and a Leica HCX PL APO CS 63x/1.32 oil immersion objective at the Leica.

For the two-photon experiments we initially used the Zeiss LSM 510 NLO microscope (beam splitter: HFT KP 700/488; filter: LP545) coupled to a Ti:Sapphire laser (Mira 900, Coherent) and later a custom-built setup that was coupled to a Ti:Sapphire laser (Mira 900F, Coherent) equipped with special cavity mirrors that allowed tuning to wavelengths of up to 1050 nm.

In the custom microscope the fluorescence was filtered first with an IR-blocking heat mirror (Calflex-X, Linos AG, Göttingen, Germany) then a long-pass filter LP530 (AHF analysentechnik, Tübingen, Germany). The approximate average powers of the mode-locked laser at the sample were: 7.5 mW for 1040 nm, 5 mW for 1000 nm, and 4 mW for 960 nm. For all two-photon measurements we used a Zeiss IR 40x/0.8 water immersion objective. In the custom two-photon measurement setup fluorescence light was detected using GaAsP photomultipliers (H7422P-40mod, Hamamatsu).

Line scans were oriented across (Fig. 2) or tangential to (Fig. 3 and 4) the cell studied. Care was always taken to orient the polarization of the excitation light perpendicular to the membrane to ensure alignment with the absorption dipole of the dye. The temporal resolution was ~1 ms (0.96 ms per line for the Zeiss microscope and 1.00 ms for both the Leica microscope and for the custom two-photon measurement). During the line scan we applied voltage pulses (10 ms duration spaced by 10 ms pauses) with opposite polarities to the silver-wires, at first in an increasing then in a decreasing order (Fig. 1 *d*). The total voltages were 12, 24, and 36 V, which, given a wire spacing of 2.4 mm, correspond to electric field strengths of 5 mV/μm, 10 mV/μm and 15 mV/μm. After collecting data at the different excitation wavelengths 3-D stacks of the cells were taken. All measurements were shot-noise limited. This was explicitly confirmed for the Zeiss and the custom two-photon measurements by the linear dependence of the variance on the mean fluorescence intensity.

ANALYSIS

All line scans were background corrected by subtraction of a value resulting from an averaged time trace outside the cell. We didn't correct for bleaching, which was almost imperceptible. Multiple experiments on the same cell and with the same excitation wavelength were usually averaged before calculating relative changes in fluorescence (ΔF/F). As resting fluorescence (f) we used the mean of the 20 data
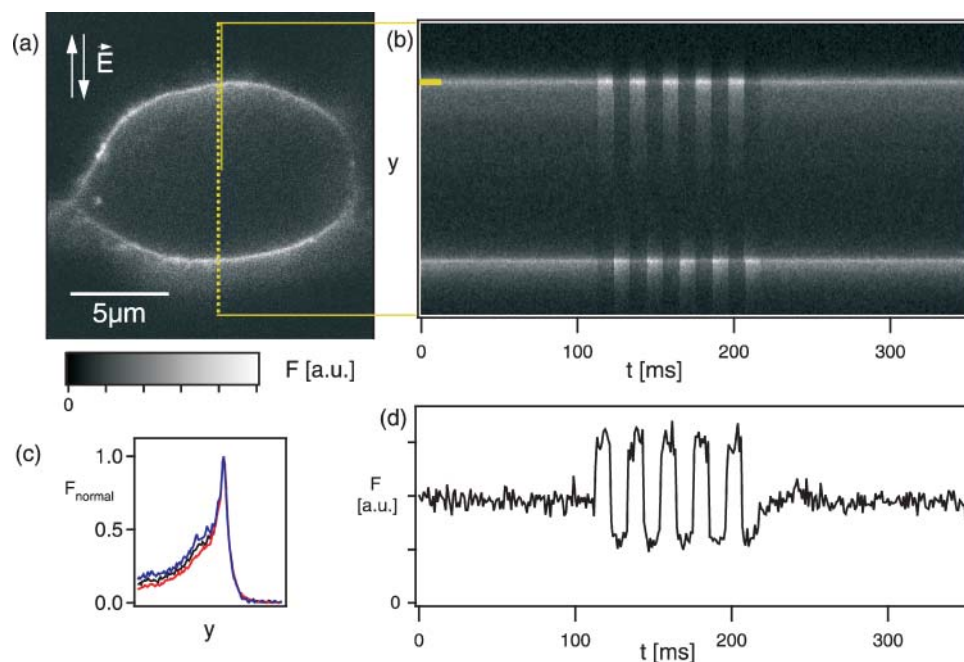
FIGURE 2 (*a*) Fluorescence of an ANNINE-6 stained HEK293 cell scanned in XY direction. A line scan was acquired at the dotted line. The lipophilic dye shows a high membrane affinity. The preferred dipole moment orientation along the membrane normal causes brighter fluorescence parallel to the laser polarization (*vertical*). (*b*) During the line scan we applied alternating external electric field pulses to show the opposing fluorescence changes on opposite cell sides. The change of membrane potential on each side was ~ ±110 mV. The 514 nm Ar-ion laser line was used for excitation. (*c*) The external electric fields cause no movement artifact: The average of 50 lines from the upper membrane in (*b*) (position marked in *a* by *solid yellow line*) without external electric field (*black line*) and both external electric field directions (*red* and *blue line*) were all normalized to their intensity maximum and superimposed. (*d*) The average of four time traces marked yellow in *b* show the signal-to-noise ratio of this single trial measurement.

points before the beginning of the voltage stimulus. To get ΔF values we averaged the central 8 data points during the pulse, which is 10 points long, and then subtracted the mean of the values (each calculated correspondingly) for the preceding and following interpulse intervals. We only considered measurements from cells where fluorescence responses were still present after measurements with a complete wavelength set had been performed and the 3-D stack was taken.

RESULTS

One-photon excitation

To validate the trans-cellular field stimulation method, we first performed responsivity measurements using wavelength (458 nm, 488 nm) for which the sensitivity has been published (Kuhn and Fromherz, 2003). We find reasonable agreement (488 nm: −0.28%/mV in HEK293 compared to −0.29%/mV in Leech). We then proceeded to use a wavelength (514 nm) more toward the long edge of the absorption spectrum to test whether the sensitivity increases further toward longer wavelengths. To rule out spurious signals that might be created as the result of movement, for example, caused by external electric field-induced ionophoresis or heating, we scanned through cells parallel to the applied field and perpendicular to the cell membrane (Fig. 2). No lateral movement was seen of the cell membrane on either side of the cells, as is evident from the straightness of the bright lines in the line scan (Fig. 2 *b*) and can be more closely examined

by looking at the normalized plots of intensities along the scan line averaged over the 0, −110 mV and +110 mV stretches of the line scan (Fig. 2 *c*). Here, as in all experiments, the laser polarization was aligned with the absorption dipole of the dye, which has for comparable dyes been measured to be oriented largely perpendicular to the membrane (Visser et al., 1995; Lambacher and Fromherz, 2001). Further evidence for the orientation of the absorption dipole is the variation of the fluorescence intensity around the cell (Fig. 2 *a*) with minima at the 3 and 9 o'clock positions, where the polarization is parallel to the membrane. As expected with trans-field stimulation, the electric field on opposite sides of the cell points at the same absolute direction but in opposite direction relative to the dye molecules in the outer leaflet of the membrane bilayer. The signals, therefore, have different directions on opposite sides of a cell (Fig. 2 *b*). The voltage resolution in single-trial measurements with 1 ms temporal resolution was ~12 mV rms (Fig. 2 *d*).

To increase the number of scan-line pixels on the membrane, all further measurements were performed with the scan line tangential to the cell. The laser polarization, of course, was kept parallel to the electric field (Fig. 3). The image of a typical cell is shown in Fig. 3 *a*. An XZ scan (Fig. 3 *b*) reveals that only little fluorescence is generated inside the cell. One problem when using trans-cellular stimulation is that the actual voltage drop across the membrane depends on the cellular geometry and the estimation of precise values for the voltage drop across a particular membrane would require detailed electrostatic calculations, even if the cytosol
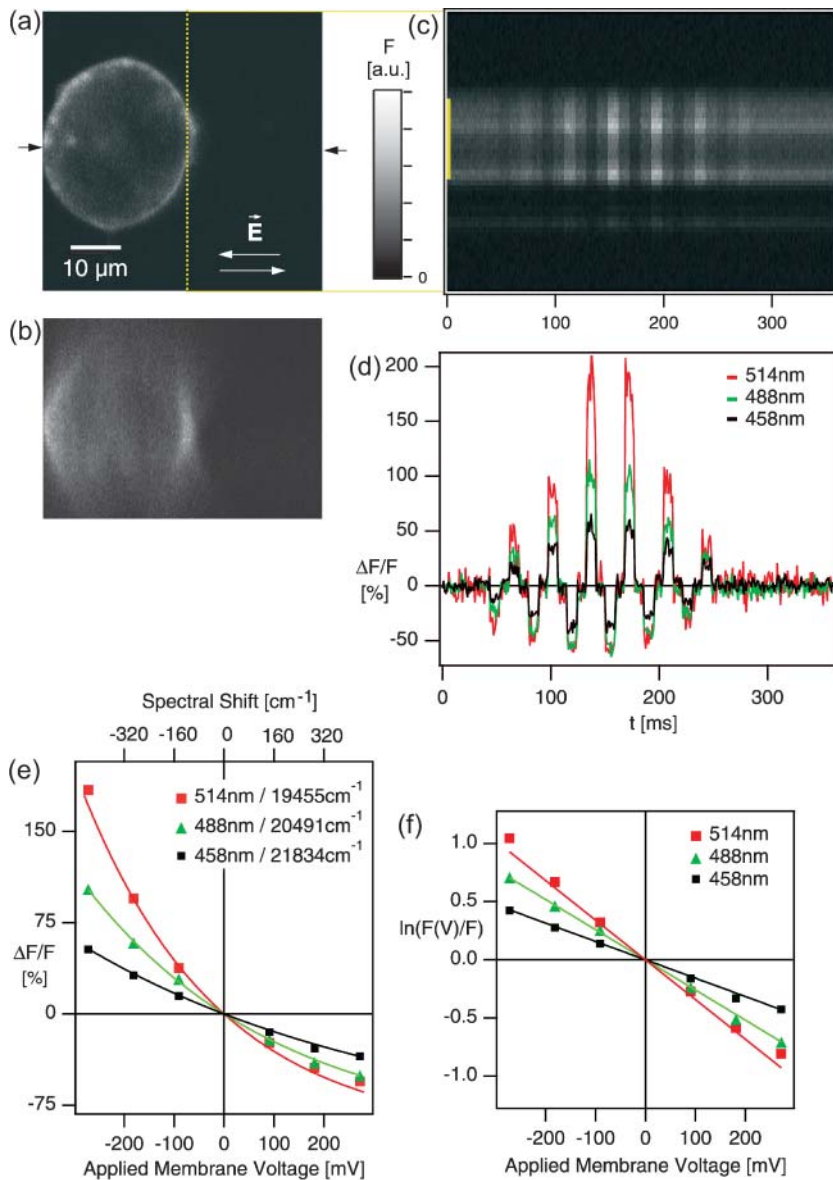
FIGURE 3 VSD signals in HEK293 cells stimulated by external electric fields. (*a*) XY fluorescence image excited at 488 nm by an Ar-ion laser. The arrows mark the position of the XZ scan shown in *b*. The dotted yellow line in *a* marks the position of the line scans. The line scans were performed perpendicular to the electric field direction and along the membrane. (*c*) The presented line scan was acquired at an excitation wavelength of 514 nm and is the average of 12 trials. (*d*) The relative fluorescence changes increase when the excitation wavelength is increased from 458 nm over 488 nm to 514 nm. The time trace at 514 nm in *d* is the average of the in *c* yellow marked traces. (*e*) The relative fluorescence changes become more nonlinear as a function of the applied membrane voltage with increasing wavelength. For the calculation of the applied membrane voltage, the diameter and a correction factor for a hemispherical cell was considered. The data points are fitted by exponential curves of the form ($e^{\alpha x} - 1$). The top scale indicates the spectral shift in wavenumbers expected from the applied membrane voltage change. (*f*) In a lin-log plot (fluorescence at an applied voltage over ''resting'' fluorescence versus membrane voltage) the data points show a quite linear relationship. The straight lines indicate $\ln(e^{\alpha x})$.

can be assumed to be isopotential. Since we were mainly interested in the wavelength dependence of the responsivity we used an approximation to calculate the membrane voltage (Gross et al., 1986). For spherical cells in free solution or for hemispherical cells sitting on a coverslip the actual transmembrane voltage is larger by a factor of 1.5 (Gross et al., 1986) than the voltage drop expected by merely taking the product of cell diameter and field strength, since the insulating cell body displaces the current flow. We also assumed the voltage drop to be equally divided between both membranes, which was confirmed for the cell in Fig. 2 by the complementary fluorescence changes seen on opposite sides of the cell. The peak membrane voltage change for the cell of Fig. 3, which has an extent of 24 μm in X direction, was thus estimated at ±90 mV for a field of ±5 mV/μm. We consider

a membrane depolarizing voltage as positive change, which results in a fluorescence decrease if the outer leaflet is stained. Alternating dimming and brightening of the fluorescence intensity can clearly be seen in the averaged line scan data (Fig. 3 *c*). Fig. 3 *d*, where we compare the fluorescence changes for different excitation wavelengths (458 nm, 488 nm, and 514 nm), clearly demonstrates the increase of the responses toward longer wavelengths. As expected, the fluorescence followed the applied voltage instantaneously.

Relative fluorescence changes are plotted as a function of membrane voltage in Fig. 3, *e* and *f*. Because ANNINE-6 is a pure Stark-shift probe, it is also possible to translate the membrane voltage change directly into a spectral shift (Fig. 3 *e*, *top scale*). The responses become increasingly nonlinear

at longer excitation wavelengths, deviating at 514 nm from linearity by factors of ~0.66 and 1.5 at +180 mV and −180 mV, respectively. If the excitation spectrum follows an exponential function (at least locally), the voltage dependence can be approximately linearized by using the logarithm of $F(V)/F (V = 0)$, as is shown in Fig. 3 f. The slope sensitivities (α) at the resting potential can be calculated either by fitting ($e^{\alpha x} − 1$) to the data in Fig. 3 e or by using the line slopes in Fig. 3 f. For the cell shown in Fig. 3 a we find −0.16%/mV, −0.26%/mV, and −0.37%/mV for wavelengths of 458 nm, 488 nm, and 514 nm, respectively. The mean sensitivities (four cells measured) at these wavelengths are −0.16 ± 0.02%/mV, −0.28 ± 0.03%/mV, and −0.35 ± 0.03%/mV, respectively.

To test our assumption about the extracellular stimulation the sensitivity at 514 nm was tested by controlling the membrane voltage directly using tight-seal whole-cell recordings of HEK293 cells (Fig. 4). The mean sensitivity measured in four cells using voltage jumps of ±25, ±50, and ±75 mV is −0.37 ± 0.02%/mV, in agreement with the results achieved by the external electric field method.

Two-photon excitation

We proceeded to measure the voltage sensitivities under two-photon excitation. Images show very low intracellular background (Fig. 5, a and b) with the reduction compared to the ''confocal'' microscope (with an open pinhole used in Fig. 3), likely due to better out-of-focus discrimination. The long wavelength edge of the two-photon excitation spectrum is expected to resemble that of the one-photon spectrum because in molecules with a large change in dipole moment, the lowest one-photon transition is also strongly two-photon allowed (Dick and Hohlneicher, 1982). Initial experiments at 976 nm showed that with two-photon excitation the sensitivity was slightly higher (by ~20%) than with

one-photon excitation at half the wavelength (488 nm), measured in the same cell. To confirm the increase toward the very edge of the spectrum we performed measurements at 960 nm, 980 nm, 1000 nm, 1020 nm, and 1040 nm (Fig. 5). As for one-photon excitation the voltage dependence of the fluorescence signals became more sensitive and nonlinear with increasing excitation wavelength (Fig. 5 e). The slope sensitivities for this cell at the resting potential were −0.35%/mV, −0.41%/mV, −0.49%/mV, −0.54%/mV, and −0.59%/mV at 960 nm, 980 nm, 1000 nm, 1020 nm, and 1040 nm, respectively (Fig. 5, e and f). The mean sensitivities (4 cells) were −0.29 ± 0.05%/mV, −0.35 ± 0.05%/mV, −0.43 ± 0.05%/mV, −0.47 ± 0.06%/mV and −0.52 ± 0.06%/mV, respectively. To test whether the rather high excitation intensities needed to excite sufficient fluorescence so far off the peak do damage the cells more than excitation at the peak of absorption, where the intensities required to get the same amount of fluorescence are much smaller, we exposed the same location in a single cell to hundreds of line scans. The cell, shown in Fig. 5, responded with undiminished amplitude (begin: −0.59 ± 0.01%/mV, end: −0.58 ± 0.02%/mV) after 900 line scans had been performed (with excitation at 1040 nm) over a period of over 2 h. These line scans represent ~350,000 individual voltage measurements each with an rms resolution of ~25 mV.

DISCUSSION

We have shown that when excited near the long wavelength edge of the absorption spectrum Stark-shift VSDs can show very large fractional sensitivities. This was specifically tested using ANNINE-6, which is one of a series of improved derivatives of the earlier voltage-sensitive hemicyanine dyes (Grinvald et al., 1983; Fluhler et al., 1985; Ephardt and
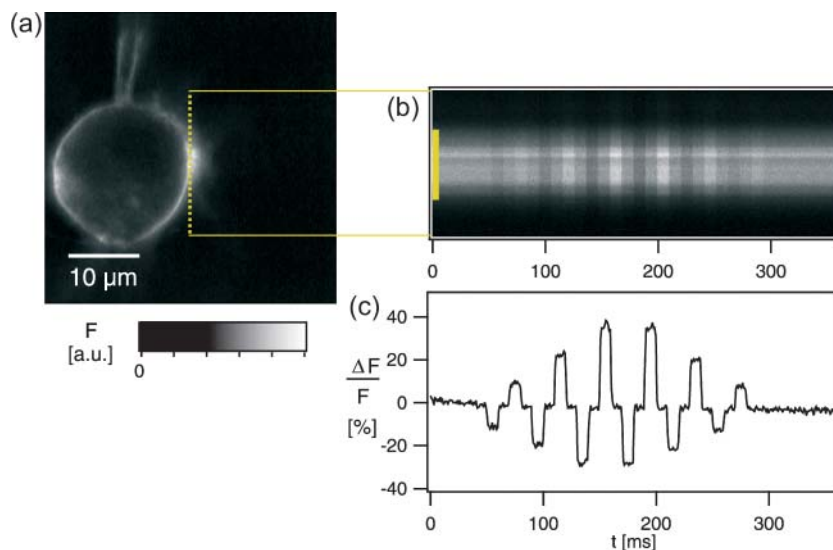

FIGURE 4 Sensitivity of ANNINE-6 at an excitation wavelength of 514 nm, in a voltage-clamped HEK293 cell. (a) XY scan of the cell (note patch electrode) excited at 514 nm. The position of the line scan is marked with yellow dots. (b) Line scan of the same cell with voltage steps to ±25 mV, ±50 mV, and ±75 mV. Four line scans were averaged. (c) The trace of the relative fluorescence change is the spatial average along the yellow bar in b.
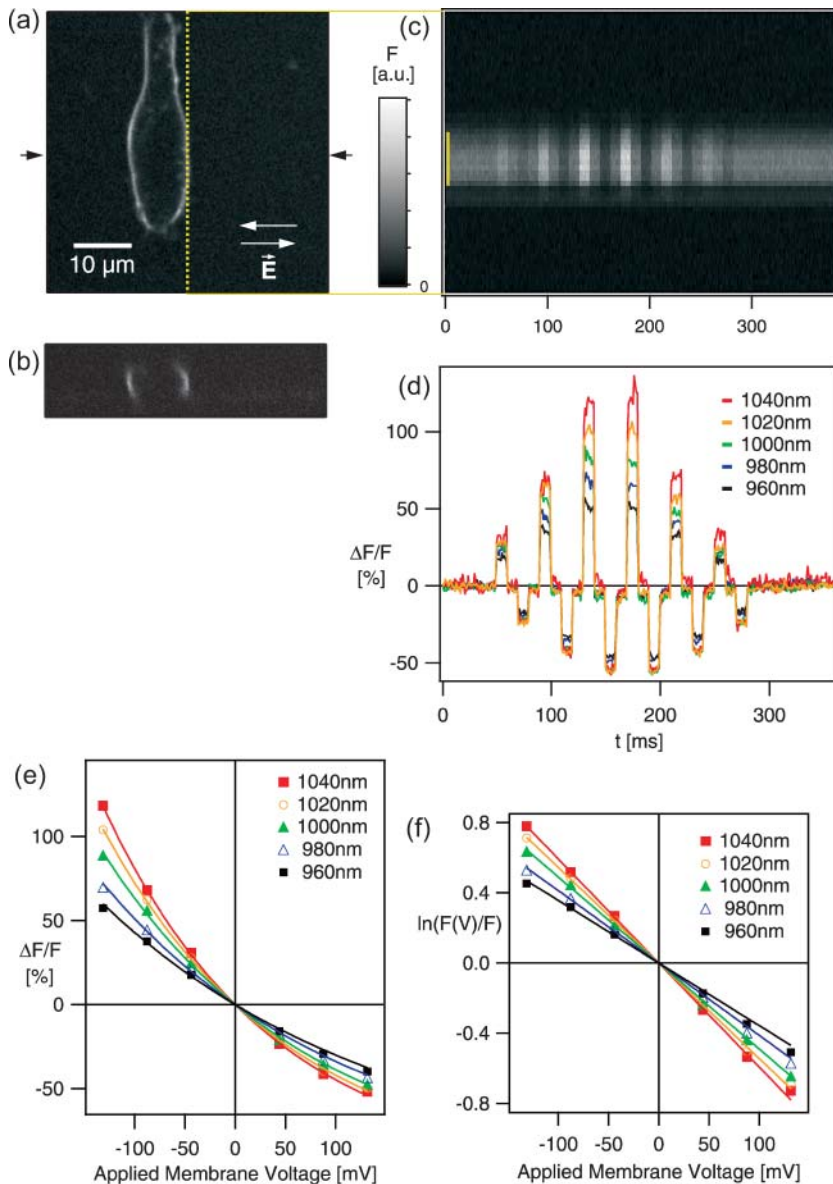
FIGURE 5 Signals from HEK293 cells stained with ANNINE-6, excited by two-photon absorption and stimulated by an extracellular electric field. (*a*) XY scan and (*b*) XZ scan of a cell (excitation at 1040 nm). (*c*) Line scan excitation was at 1040 nm, the orientation of the electric field is given by arrows (average of 12 trials). (*d*) The fluorescence changes for wavelengths between 960 nm to 1040 nm. The 1040 nm time trace is the spatial average of the data in *c*. (*e*) Relative fluorescence changes versus applied membrane voltage with exponential fits. (*f*) Same data as *e* plotted on a lin-log scale.

Fromherz, 1993) that are particularly well suited for this method due to their large charge shift.

Sensitivities in different cell types, comparison of one-photon and two-photon excitation

Because the voltage sensitivities of many VSDs are strongly cell-type dependent (Ross and Reichardt, 1979; Loew et al., 1992; Spors and Grinvald, 2002), we compared the sensitivities for ANNINE-6 in Retzius cells of the leech, measured by Kuhn and Fromherz (2003) with those we found in HEK293 cells (Fig. 6 *b*). Lack of cell-type dependence is desirable, since it allows calibrated voltage recordings even in unknown cells and preparations, and was expected from the pure Stark-effect character (Kuhn and Fromherz, 2003) of the ANNINE dye. At wavelengths of

458 nm and 488 nm the sensitivities agree within the measurement uncertainty. Even for 514 nm, where the measurements in leech neurons were thought to be flawed due to low fluorescence intensity and closeness to the beam splitter edge (Kuhn and Fromherz, 2003; and Kuhn and Fromherz, personal communication), both sensitivity values agree. The agreement of sensitivities taken with unpolarized light (Kuhn and Fromherz, 2003) and our measurements (with polarized laser excitation) also suggests that there are no significant sensitivity improvements with polarized excitation (this may be different in the two-photon case, see below). The main part of the spectrum and the calculated sensitivities are well fit by a log-normal function (Siano and Metzler, 1969; Kuhn and Fromherz, 2003). However, for the longer wavelengths (>480 nm, <21000 cm^{-1}) we find that the sensitivities both in leech and HEK293 cells start to
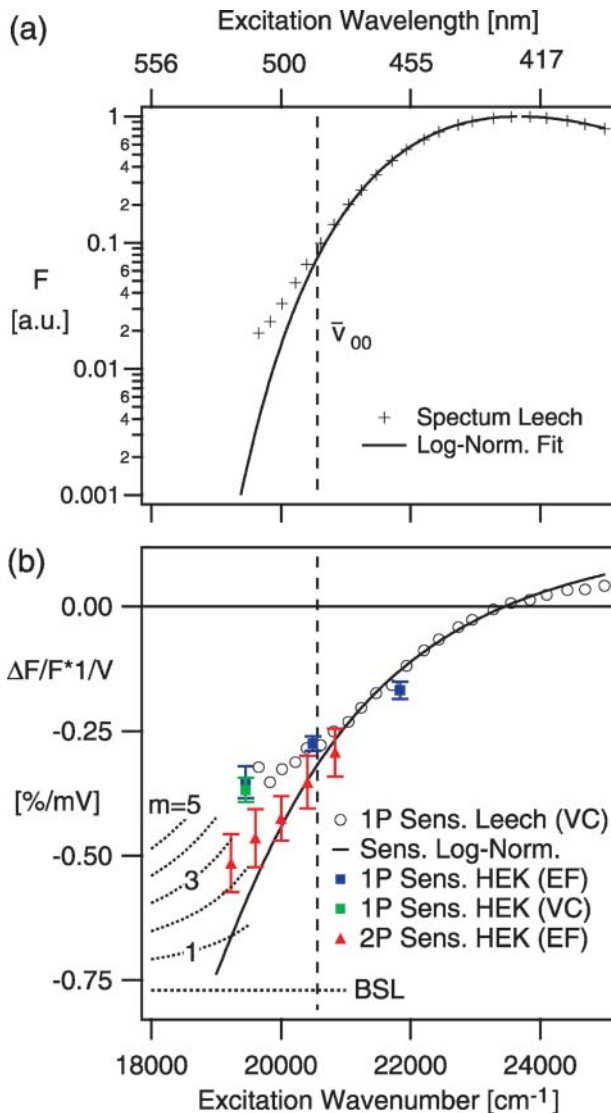
FIGURE 6 Excitation spectrum (*a*) and sensitivity (*b*) of ANNINE-6 near the red edge. (*a*) Data from a leech neuron (*crosses*) were fitted with a log-normal function (*line*) (data from Kuhn and Fromherz, 2003). (*b*) The sensitivity expected from the shift of the log-normal spectrum (*line*) and the measured leech sensitivities (*open circles*, data from Kuhn and Fromherz, 2003). Averaged slope sensitivities ($n = 4$, mean $\pm$ SD) found in HEK293 cells in our study with one-photon excitation (*blue squares*, external electric field method; *green square*, voltage-clamp) and with two-photon excitation (*red triangles*, external electric field method). For two-photon excitation, the data are plotted versus the excitation energy, i.e., twice the laser wavenumber. $\bar{\nu}_{00}$ is indicated by the dashed vertical lines in *a* and *b*, the Boltzmann sensitivity limit BSL for ANNINE-6 as dotted horizontal line in *b*. Dotted curved lines in *b* indicate expected sensitivities using multiple vibrational modes $m + 1$ ($m = 1\ldots5$).

deviate (Fig. 6) from those expected for the log-normal function (fitted globally). The two-photon sensitivities show the same trend. However, the measured sensitivities are generally larger with two-photon excitation than with one-photon excitation. In the one case, where the one-photon and two-photon sensitivities were measured for the same cell for

wavelengths of 488 nm and 976 nm, respectively, the two-photon values were ~20% higher. The two-photon sensitivities may, in fact, more closely reflect the actual ''molecular'' sensitivities due to the lower background, better optical sectioning (open pinhole with one-photon excitation), and better orientational selectivity of two-photon excitation (Lakowicz et al., 1992). The nonlinearity of the sensitivity curves at the spectral edge reflects the curvature of the spectrum at the excitation wavelength.

Sensitivity of VSD recordings

Since fluorescence measurements in living tissue in general and VSD measurements in particular are always limited by photodamage, it is crucial to carefully explore the optimization of excitation and detection spectral ranges. Optimization can be performed as described for the general case (Kuhn and Fromherz, 2003). In the absence of background fluorescence and if there are no limits on the excitation (both in terms of spectra and power density), rather straightforward, simplified rules can be established.

Since the generation of fluorescence photons requires molecular excitation, which is also the source of photobleaching and photodamage, it is crucial to maximize the information gained per molecular excitation, i.e., per generated (not detected) fluorescence photon. This distinction between generated and detected photons is important since large fractional intensity changes can sometimes be achieved by detecting only in a small wavelength band, at the expense of discarding a large fraction of the total fluorescence generated. Let us first assume that the excitation is by a collection of wavelengths. The response function is then the sum of response functions for each of the excitation wavelengths and, obviously, shifting excitation energy to wavelengths with better response will increase the total SNR. An optimal value will be reached when all excitation occurs for the wavelength with the best response. This shows that monochromatic illumination at the appropriate wavelength is optimal, i.e., at least as good as illumination with any collection of wavelengths. To get simpler expressions we henceforth use an energy-proportional scale, i.e., wavenumbers. For a pure Stark-shift probe, for which the wavenumber dependent spectra can be written as $\varepsilon(\bar{\nu}_{ex}, V) = \varepsilon_0(\bar{\nu}_{ex} + \kappa V)$ and $f(\bar{\nu}_{ex}, V) = f_0(\bar{\nu}_{ex} + \kappa V)$, the fractional change S_V in fluorescence as a function of excitation $\bar{\nu}_{ex}$ and emission $\bar{\nu}_{em}$ wavenumbers is then (Kuhn and Fromherz, 2003)

$$S_V(\bar{\nu}_{ex}, \bar{\nu}_{em}) = \kappa \left(\frac{1}{\varepsilon(\bar{\nu}_{ex})} \frac{d\varepsilon(\bar{\nu}_{ex})}{d\bar{\nu}_{ex}} + \frac{1}{f(\bar{\nu}_{em})} \frac{df(\bar{\nu}_{em})}{d\bar{\nu}_{em}} \right). \quad (1)$$

The dye-specific constant κ is given by the ratio of spectral shift $d\bar{\nu}_{ex,em}$ per membrane voltage change dV, $\varepsilon(\bar{\nu}_{ex})$ is the absorption cross section and $f(\bar{\nu}_{em})$ is the quantum spectrum

of fluorescence. To optimally extract information from this spectrum we would have to detect each emission wavenumber separately and form a properly weighted average (Kuhn and Fromherz, 2003) since the voltage information that a photon provides depends on its wavenumber. The voltage sensitivity (Eq. 1) consists of two terms, one term that results from the voltage dependence of the excitation spectrum and the other one from the voltage dependence of the emission spectrum. For excitation at the spectral edge however, this function is dominated by the excitation sensitivity as $|\varepsilon'(\bar{\nu}_{ex})/\varepsilon(\bar{\nu}_{ex})|$ strongly increases toward the edge. Almost all emitted photons, independent of their wavenumber, yield a voltage signal with the same sign and with similar magnitude for the majority of the light. This is rather convenient since it makes the voltage variance almost independent of the emission wavelength for most of the emitted photons (except at for a small fraction at the very edge of the emission spectrum) and thus allows combining photons with equal weight, allowing near optimal detection with a single detector. The pure excitation voltage sensitivity $\langle S_V(\bar{\nu}_{ex})\rangle$ can now be expressed as

$$\langle S_V(\bar{\nu}_{ex})\rangle = \kappa \frac{1}{\varepsilon(\bar{\nu}_{ex})} \frac{d\varepsilon(\bar{\nu}_{ex})}{d\bar{\nu}_{ex}}. \qquad (2)$$

An important parameter is the number of photons n needed to detect a certain voltage change ΔV. With shot-noise limited detection the voltage-induced fluorescence change $\langle S_V(\bar{\nu}_{ex})\rangle \Delta V$ has to overcome the relative noise signal N given by

$$N = \frac{\sqrt{n}}{n}. \qquad (3)$$

So the number of photons necessary to detect a given fluorescence change can be calculated by

$$\langle S_V(\bar{\nu}_{ex})\rangle \Delta V \geq \frac{1}{\sqrt{n}}. \qquad (4)$$

In the case of ANNINE-6 the voltage sensitivity for excitation at, for example, 458 nm is $-0.17\%/mV$, which means that a voltage change of 10 mV could be detected with 3500 photons whereas 350,000 detected photons allow a voltage estimate with a standard deviation of 1 mV. With an excitation wavelength of 514 nm and a sensitivity of $-0.35\%/mV$ the number of photons to detect voltage changes of 10 mV and 1 mV are 820 and 82,000, respectively.

Fig. 6 *b* shows the sensitivity $\langle S_V(\bar{\nu}_{ex})\rangle$ as a function of excitation wavelength. To obtain a given accuracy one has to detect a certain number of photons. Therefore, the sensitivity is a direct measure for the number of voltage measurements of a given sensitivity one can make with a fixed number of photons before, for example, the sample bleaches or is

photodamaged. This illustrates the advantage gained from excitation at the spectral edge, provided, of course, the damage per molecular excitation is wavelength independent. This is an issue that will have to be explored further.

Maximal theoretical sensitivity and explanation of tail sensitivity

A common approximation used for spectral shapes is the log-normal function (Siano and Metzler, 1969), which would imply an ever-increasing, in fact, diverging sensitivity toward longer wavelengths and the vanishing of excitation above a wavelength of 591 nm. However, simple considerations predict a tail in the absorption spectrum F that follows a Boltzmann distribution (Hinshelwood, 1940)

$$F = F_0 e^{-\frac{E}{k_B T}}, \qquad (5)$$

because an electronic transition between the ground and the excited state with the energy difference $h\bar{\nu}_{00}c$ (h Planck constant, $\bar{\nu}_{00}$ wavenumber of the 00 transition, c light velocity) and an excitation energy $h\bar{\nu}c$ ($\bar{\nu}$ wavenumber of excitation), which is assumed to be below $h\bar{\nu}_{00}c$, requires additional vibrational energy $E = h\bar{\nu}_{00}c - h\bar{\nu}c$ to reach the lowest excited state, in analogy to anti-Stokes lines in scattering theory. The absorption F is then proportional to the fraction of molecules with higher vibrational energy than E. Since for ANNINE-6 $\bar{\nu}_{00}$ is 20,565 cm^{-1} (486 nm) (Kuhn and Fromherz, 2003) most of the wavelengths we used here are, in fact, in the spectral tail. For a pure Stark-effect dye, implying a mere shift in the spectrum, the excitation efficiency then changes for small changes in the voltage ΔV by

$$\left(\frac{\Delta F}{F}\right)_{Max} = e^{-\frac{\Delta \mu \Delta V \cos\vartheta}{d} \frac{1}{k_B T}} - 1 = e^{-\frac{\Delta E}{k_B T}} - 1 \overset{\Delta E \ll k_B T}{\approx} -\frac{\Delta E}{k_B T}, \quad (6)$$

for excitation in the Boltzmann tail ($\Delta \mu$ is the intramolecular charge displacement upon electronic excitation, d is the membrane thickness, ϑ is the angle between charge displacement and membrane normal). This is the maximal relative change possible for a given change in charge shift (change in dipole moment) at a certain temperature. For ANNINE-6 the shift is 1.6 cm^{-1}/mV (Kuhn and Fromherz, 2003), which translates into a Boltzmann-tail sensitivity of $-0.77\%/mV$. For comparison: the highest measured sensitivity value was $-0.52 \pm 0.05\%/mV$ (with two-photon excitation at 1040 nm, corresponding to 520 nm). Because this sensitivity limit depends only on the shift of the excitation spectrum the expected sensitivity limit for other dyes should be lower (ANNINE-5: 1.3 cm^{-1}/mV; BNBIQ: 1.0 cm^{-1}/mV; di-4-ANEPBS: 0.9 cm^{-1}/mV; RH-421: 0.5 cm^{-1}/mV; Kuhn and Fromherz, 2003).

A more realistic description of the spectral sensitivity predicts a flattening of the spectral tail compared to the

Boltzmann curve as more vibrational modes (m+1) are taken into account (Hinshelwood, 1940)

$$F = F_0 e^{-\frac{E}{k_B T}} \sum_{p=0}^{m} \frac{(E/k_B T)^p}{p!}. \qquad (7)$$

This approach was, for example, used successfully to describe the long wavelength spectral tail of visual pigments (Lewis, 1955; Voss and Van Norren, 1984). Fig. 5 *b* includes curves for $m = 1$ to 5 and suggests that 3 or 4 vibrational modes are relevant for ANNINE-6. To really test, however, whether the multiple levels or residual background are responsible for the deviation from the log-normal behavior measurements at even longer wavelengths would be necessary.

In practice a major limitation is the availability of sufficiently intense light sources since, as this article shows, the optimal excitation wavelengths will almost always lie in a low absorption part of the spectrum. Furthermore, the range over which the excitation wavelength is nearly optimal, is typically narrow and does usually not coincide with a strong spectral line. Therefore, one has to resort to using a narrow spectral band and hence only a small fraction of the total light output from a broad spectrum light source such as an arc or an incandescent bulb. The use of lasers, which can provide narrow-band excitation, for wide-field illumination is beset by speckle problems and often a line at the appropriate wavelength is not available. A further problem can be the excitation of tissue auto fluorescence as increasingly intense light is used for excitation.

Although we have only tested extreme red excitation on one dye (ANNINE-6) it should be applicable to all spectral shift dyes with a sufficiently steep long-wavelength spectral fall-off.

REFERENCES

Denk, W., J. H. Strickler, and W. W. Webb. 1990. 2-photon laser scanning fluorescence microscopy. *Science.* 248:73–76.

Dick, B., and G. Hohlneicher. 1982. Importance of initial and final-states as intermediate states in 2-photon spectroscopy of polar-molecules. *J. Chem. Phys.* 76:5755–5760.

Ephardt, H., and P. Fromherz. 1993. Fluorescence of amphiphilic hemicyanine dyes without free double-bonds. *J. Phys. Chem.* 97:4540–4547.

Fluhler, E., V. G. Burnham, and L. M. Loew. 1985. Spectra, membrane binding, and potentiometric responses of new charge shift probes. *Biochemistry.* 24:5749–5755.

Grinvald, A., A. Fine, I. C. Farber, and R. Hildesheim. 1983. Fluorescence monitoring of electrical responses from small neurons and their processes. *Biophys. J.* 42:195–198.

Grinvald, A., R. D. Frostig, E. Lieke, and R. Hildesheim. 1988. Optical imaging of neuronal activity. *Physiol. Rev.* 68:1285–1366.

Gross, D., L. M. Loew, and W. W. Webb. 1986. Optical imaging of cell membrane potential changes induced by applied electric fields. *Biophys. J.* 50:339–348.

Hinshelwood, C. N. 1940. The Kinetics of Chemical Change. Clarendon Press, Oxford.

Hübener, G., A. Lambacher, and P. Fromherz. 2003. Anellated hemicyanine dyes with large symmetrical solvatochromism of absorption and fluorescence. *J. Phys. Chem. B.* 107:7896–7902.

Kuhn, B., and P. Fromherz. 2003. Anellated hemicyanine dyes in a neuron membrane: molecular stark effect and optical voltage recording. *J. Phys. Chem. B.* 107:7903–7913.

Lakowicz, J. R., I. Gryczynski, Z. Gryczynski, E. Danielsen, and M. J. Wirth. 1992. Time-resolved fluorescence intensity and anisotropy decays of 2,5-diphenyloxazole by 2-photon excitation and frequency-domain fluorometry. *J. Phys. Chem.* 96:3000–3006.

Lambacher, A., and P. Fromherz. 2001. Orientation of hemicyanine dye in lipid membrane measured by fluorescence interferometry on a silicon chip. *J. Phys. Chem. B.* 105:343–346.

Lewis, P. R. 1955. A theoretical interpretation of spectral sensitivity curves at long wavelength. *J. Physiol.-London.* 130:45–52.

Loew, L. M. 1982. Design and characterization of electrochromic membrane probes. *J. Biochem. Biophys. Meth.* 6:243–260.

Loew, L. M., L. B. Cohen, J. Dix, E. N. Fluhler, V. Montana, G. Salama, and J. Y. Wu. 1992. A naphthyl analog of the aminostyryl pyridinium class of potentiometric membrane dyes shows consistent sensitivity in a variety of tissue, cell, and model membrane preparations. *J. Membr. Biol.* 130:1–10.

London, J. A., D. Zecevic, and L. B. Cohen. 1987. Simultaneous optical recording of activity from many neurons during feeding in Navanax. *J. Neurosci.* 7:649–661.

Meyer, E., C. O. Muller, and P. Fromherz. 1997. Cable properties of dendrites in hippocampal neurons of the rat mapped by a voltage-sensitive dye. *Eur. J. Neurosci.* 9:778–785.

Ross, W. N., and L. F. Reichardt. 1979. Species-specific effects on the optical signals of voltage-sensitive dyes. *J. Membr. Biol.* 48:343–356.

Salinas, E., and T. J. Sejnowski. 2001. Correlated neuronal activity and the flow of neural information. *Nat. Rev. Neurosci.* 2:539–550.

Siano, D. B., and D. E. Metzler. 1969. Band shapes of electronic spectra of complex molecules. *J. Chem. Phys.* 51:1856–1861.

Singer, W. 1999. Neuronal synchrony: a versatile code for the definition of relations? *Neuron.* 24:49–65.

Spors, H., and A. Grinvald. 2002. Spatio-temporal dynamics of odor representations in the mammalian olfactory bulb. *Neuron.* 34:301–315.

Visser, N. V., A. Vanhoek, A. J. W. G. Visser, J. Frank, H. J. Apell, and R. J. Clarke. 1995. Time-resolved fluorescence investigations of the interaction of the voltage-sensitive probe Rh421 with lipid-membranes and proteins. *Biochemistry.* 34:11777–11784.

Voss, J. J., and W. A. Van Norren. 1984. Limits of the visual spectrum. *In* Limits in Perception. A. J. Doorn, W. A. Van de Grind, and J. J. Koenderink, editors. VNU Science Press, Utrecht, The Netherlands. 69–84.